Chemistry & Biology
Article

Preferential Uptake of L- versus D-Amino Acid Cell-Penetrating Peptides in a Cell Type-Dependent Manner

Wouter P.R. Verdurmen,[1] Petra H. Bovee-Geurts,[1] Parvesh Wadhwani,[2] Anne S. Ulrich,[2] Mattias Hällbrink,[3] Toin H. van Kuppevelt,[1] and Roland Brock[1,*]
[1]Department of Biochemistry, Nijmegen Centre for Molecular Life Sciences, Radboud University Nijmegen Medical Centre, 6525 GA Nijmegen, The Netherlands
[2]Institute for Biological Interfaces (IBG-2), Institute of Organic Chemistry, and Center for Functional Nanostructures, Karlsruhe Institute of Technology, 76131 Karlsruhe, Germany
[3]Department of Neurochemistry, Stockholm University, S-10691 Stockholm, Sweden
*Correspondence: r.brock@ncmls.ru.nl
DOI 10.1016/j.chembiol.2011.06.006

SUMMARY

The use of protease-resistant D-peptides is a prominent strategy for overcoming proteolytic sensitivity in the use of cell-penetrating peptides (CPPs) as delivery vectors. So far, no major differences have been reported for the uptake of L- and D-peptides. Here we report that cationic L-CPPs are taken up more efficiently than their D-counterparts in MC57 fibrosarcoma and HeLa cells but not in Jurkat T leukemia cells. Reduced uptake of D-peptides co-occurred with persistent binding to heparan sulfates (HS) at the plasma membrane. In vitro binding studies of L- and D-peptides with HS indicated similar binding affinities. Our results identify two key events in the uptake of CPPs: binding to HS chains and the initiation of internalization. Only the second event depends on the chirality of the CPP. This knowledge may be exploited for a stereochemistry-dependent preferential targeting of cells.

INTRODUCTION

The use of cell-penetrating peptides (CPPs) such as nona-arginine (R9), TAT, and penetratin as delivery vectors for molecules that otherwise do not cross the plasma membrane is gaining significance in biomedicine (Järver et al., 2010). Although different strategies are pursued for the optimization of CPP-based delivery, premature degradation of CPPs before they reach their target in vivo remains a common concern for therapeutic applications (Patel et al., 2007). The relevance of this concern is exemplified by the rapid degradation of CPPs when they are in contact with various cell lines (Tréhin et al., 2004; Lindgren et al., 2004; Palm et al., 2007) or when they are exposed to serum (Elmquist and Langel, 2003; Pujals et al., 2007). A common strategy to combat this issue is to employ CPPs consisting of D-amino acids (D-CPPs). The altered stereochemistry of peptides containing D-amino acids renders D-CPPs much more protease resistant than their L-amino acid counterparts (Elmquist and Langel, 2003; Pujals et al., 2007; Youngblood et al., 2007). The increased stability in serum is not limited to peptides composed entirely of D-amino acids, but was also observed for partial D-amino acid substitutions at the termini in small peptides (Tugyi et al., 2005) and for CPPs conjugated to morpholino-nucleotide oligomers (Youngblood et al., 2007).

For penetratin, uptake was observed for the reverse L-amino acid sequence, the D-peptide, and a retro-inverso analog, suggesting that backbone chirality is not important for uptake of this CPP (Brugidou et al., 1995; Derossi et al., 1996). Because uptake was also observed at 4°C, the authors suggested that internalization occurred via a receptor-independent mechanism, most likely involving direct interactions with membrane phospholipids (Derossi et al., 1996). Later studies corroborated this hypothesis for inverso and retro-inverso analogs of polyarginines and the arginine-rich TAT peptide (Mitchell et al., 2000; Wender et al., 2000), which together have led to the prevailing paradigm that cellular uptake of CPPs is a chirality-independent process. Studies using these and other CPPs, including pVEC and sweet arrow peptide, provided additional support for this current paradigm (Elmquist and Langel, 2003; Fretz et al., 2007; Pujals et al., 2008). A higher uptake efficiency of D-TAT and D-polyarginines in the presence of serum (Wender et al., 2000) was attributed to an increased proteolytic stability (Tünnemann et al., 2008).

Although the available studies thus appear to sketch a uniform picture, one should realize that these studies were conducted with a rather limited number of cell types. It is well established, however, that different mechanisms for CPP uptake are operating in different cell types (Mueller et al., 2008). Moreover, some of the earlier studies did not distinguish between membrane-bound and internalized peptides. Nowadays, the distinction between internalized and membrane-associated peptides is considered a vital aspect for the quantification of CPP uptake (Burlina et al., 2005; Richard et al., 2003; Oehlke et al., 1998) and is generally accomplished by a specific modification of the membrane-bound fraction (Burlina et al., 2005; Oehlke et al., 1998) or by a trypsin and/or heparin treatment of cells. Because trypsin does not degrade D-peptides, in studies comparing the uptake of D- and L-CPPs an incubation of cells with heparin is

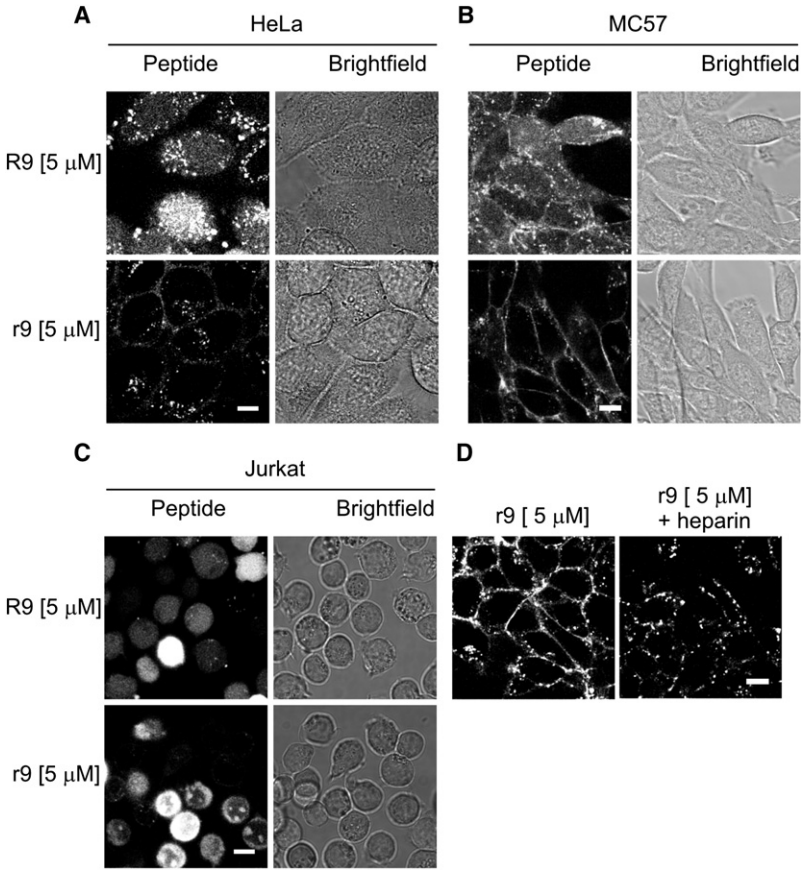

Figure 1. Cellular Distribution and Uptake of R9 and r9 in HeLa, MC57, and Jurkat Cells

(A–C) HeLa (A) and MC57 (B) cells were seeded in eight-well microscopy chambers, grown to 75% confluence, and incubated with 5 μM of peptides for 45 min. Jurkat cells (C) were similarly incubated with peptide for 45 min, washed, and then transferred into the microscopy chambers. Confocal images were acquired immediately.

(D) Illustration of the heparin-induced removal of cell-associated fluorescence of r9 in living MC57 cells. Following peptide uptake, cells were incubated twice for 5 min each with 100 μg/ml heparin.

The scale bars represent 10 μm. See also Figure S1.

the appropriate treatment for removal of membrane-bound peptides.

Recent advances in the quantification of internalization, and the introduction of protocols to study CPP uptake using live-cell confocal microscopy, warrant a new analysis of L- and D-CPP uptake. Therefore, the goal of the present study was to study in detail possible differences in the cellular uptake of arginine-rich as well as cationic amphiphilic all-L CPPs and their all-D counterparts, using a panel of cell types for which we had previously noted differences in the intracellular distribution of CPPs. The CPPs used were nona-arginine (R9), which is considered to be conformationally unstructured, and the amphiphilic CPP penetratin, which adopts different conformations depending on the local environment and also contains several arginine residues. Furthermore, the human lactoferrin-derived peptide hLF(38–59) was included (Duchardt et al., 2009). Being entirely composed of D-amino acids, the inverso peptide D-nona-arginine (r9) is at the same time also the retro-inverso analog of R9, and as such it is topologically essentially equivalent to R9 with respect to absolute side-chain orientation. For hLF, uptake efficiency is conformation dependent. Presence of a disulfide bridge is required for activity (Duchardt et al., 2009).

Surprisingly, we found significant differences in the uptake of all-L and all-D CPPs in HeLa and MC57 cells, but not in Jurkat cells. In cells with reduced uptake of D-peptides, a persistent binding to heparan sulfates (HS) was observed. These differences in uptake were restricted to uptake via endocytosis. In contrast, rapid cytoplasmic uptake by nucleation zones, which occurs for R9 and hLF at higher concentrations (Duchardt et al., 2007), was even more effective for r9. Detailed binding studies by surface plasmon resonance (SPR) and isothermal titration calorimetry (ITC) indicated that D- and L-peptides bound to HS with similar affinities, suggesting that they also bind cellular heparan sulfates with similar propensity and with similar affinities but differ in their capacity to trigger their endocytic uptake. Results obtained for a series of peptides with partial D-amino acid substitutions suggest that a consecutive stretch of L-amino acids is required to trigger uptake. The cell-type dependence of the L versus D preference suggests that the stereochemistry of cationic CPPs may be exploited as a new principle for a cell type-selective targeting.

RESULTS

Cellular Uptake of R9 and r9

To address potential differences in the cellular uptake and intracellular trafficking of CPPs (for peptide sequences, see Table S1 available online), we analyzed the uptake and intracellular distribution of R9 and r9 by confocal microscopy in MC57 fibrosarcoma (Hosaka et al., 1986), HeLa, and Jurkat cells. The selection of cell lines was motivated by previously observed differences in cytoplasmic fluorescence at low peptide concentrations, at which uptake via endocytosis occurs. In MC57 fibrosarcoma cells, fluorescence was to a larger extent cytoplasmic, whereas in HeLa cells fluorescence was more restricted to vesicular structures (Fischer et al., 2004). At low concentrations, fluorescence was also strongly cytoplasmic in Jurkat cells and other leukocytes (Fretz et al., 2007). Uptake and intracellular distribution were compared after a 45 min incubation with the peptides at a concentration of 5 μM (Figures 1A–1C).

Unexpectedly, major differences were observed in the uptake of r9 and R9 in both HeLa (Figure 1A) and MC57 (Figure 1B) cells. Punctate vesicular structures inside cells were more numerous and brighter for R9 compared to r9. Next to this punctate staining, a cytosolic fluorescence was observed for R9 but not for r9 in MC57 and, to a lesser extent, also in HeLa cells for R9. In

contrast, for r9, there was a more intense staining of the plasma membrane (Figures 1A and 1B). This staining was more pronounced for MC57 than for HeLa cells. For Jurkat cells, no membrane staining was present (Figure 1C). Instead, only differences in the intracellular localization of R9 and r9 were observed. The distribution of r9 differed from the one of R9 in that the former strongly stained the nucleoli, in accordance with previous observations (Fretz et al., 2007). Punctate fluorescent structures, indicative of endocytosis, were not observed in Jurkat cells, even when concentrations as low as 1 μM were tested.

We and others had previously described that at higher peptide concentrations, an alternative internalization mechanism occurs that rapidly leads to cytoplasmic fluorescence (Duchardt et al., 2007; Fretz et al., 2007; Verdurmen et al., 2010; Kosuge et al., 2008). Entry occurs through restricted membrane areas by an acid sphingomyelinase-dependent mechanism (Verdurmen et al., 2010). The population of cells that shows peptide entry via this mechanism can be clearly distinguished as cells with high intensity by flow cytometry. Direct cytoplasmic entry was reported to be higher for r9 compared to R9 in various cell types, including HeLa cells (Tünnemann et al., 2008). Here we also observed a much larger proportion of HeLa cells with high total fluorescence after being treated with r9 versus R9 at 20 μM (Figure S1). On the other hand, for r9, flow cytometry histograms showed the presence of cells with lower fluorescence than was observed for R9, in agreement with the microscopy data (Figure 1). These differences indicate that r9 enters more efficiently by direct cytoplasmic entry and less efficiently via endocytosis. It should be noted, however, that a quantitative determination of peptide uptake by flow cytometry may be hampered by quenching of fluorescence of fluorophores bound to cellular structures or present in acidic vesicular compartments.

Quantification of Uptake

Confocal microscopy showed a more pronounced punctate staining for R9 in comparison to r9 in MC57 and HeLa cells at a peptide concentration of 5 μM, indicative of a more efficient endocytic uptake. To quantitatively confirm these differences, a quantification method was developed based on fluorescence-correlation spectroscopy (FCS) in cell lysates in order to overcome difficulties potentially associated with fluorophore-based assays. Before lysis, cell-associated fluorescence was removed by incubation of cells with heparin (Al-Taei et al., 2006), which proved highly efficient in the removal of surface-bound fluorescence (Figure 1D). However, even after washing off all membrane-bound peptides, fluorescence intensity could be influenced by a variety of factors that may differ between R9 and r9. For instance, instead of detecting a genuine difference in peptide uptake, it was also conceivable that differences in fluorescence intensity for R9- and r9-treated MC57 cells may arise due to a higher brightness of the fluorophore when attached to R9. Moreover, quenching of fluorescence in potential peptide aggregates could affect peptide quantification. Furthermore, a fluorescein-labeled degradation product of R9 might be more strongly fluorescent than r9, for which no degradation is expected. Last, differential binding to polyanions, such as oligonucleotides or protein aggregates, could lead to the removal of intact peptides during centrifugation steps that are frequently applied in quantification protocols.

To address all of the above points, we exploited the capacity of FCS to provide information on the total fluorescence, particle number, fluorescence per molecule, and presence of aggregates (Ruttekolk et al., 2011). Nucleic acids were degraded with benzonuclease, followed by complete degradation of all proteinaceous components by proteinase K (Figure S2). When we quantified the intracellular fluorescence of R9 and r9 with the above-described protocol, the uptake of r9 was only 21% that of R9. Even when we corrected for detection efficiency (see legend of Figure S2), the uptake of r9 was still only 36% compared to uptake of R9, supporting the observation that peptide uptake is indeed more efficient for R9. Notably, also, the interaction with HS chains that will also be present in lysates did not significantly alter the fluorescence of R9 and r9 (Figure S3).

Due to the complexity of the FCS-based method, we also used a simpler fluorimetry method to assess peptide internalization. With this method, we found that uptake of r9 was 46% ± 2% that of R9 in MC57 cells, and comparable observations were made for HeLa cells (53% ± 1%), whereas no significant differences were observed in Jurkat cells (91% ± 8% r9 compared to R9).

Another factor possibly contributing to the observed differences in cellular uptake was the structural environment of the fluorophore. Because r9 corresponds to a retro-inverso R9, coupling of the fluorophore to the C terminus of r9 should even more closely mimic R9. However, very similar cellular distributions of fluorescence were found for (1) an N-terminally carboxyfluorescein-labeled and C-terminally amidated r9, and (2) an N-terminally acetylated and C-terminally amidated r9, for which the carboxyfluorescein moiety was attached to a C-terminal lysine (Fischer et al., 2003) (Figure S4A), demonstrating that the position of the fluorophore does not explain the differences in distribution and uptake between r9 and R9.

Peptide Export

Another factor that may lead to a different distribution and amount of cell-associated fluorescence is the rate of export of either the CPP or its degradation products. To investigate whether R9 or its degradation products were retained more efficiently in HeLa or MC57 cells over the 1 hr time course of the experiments, these cells were electroporated with a 5 μM solution of either R9 or r9 (Figures S4B and S4C). Electroporation delivers a pulse of peptides directly into the cytosol. Therefore, this method is well suited to follow the release kinetics of molecules. Both the images per se and the image-based quantification of the mean intracellular fluorescence illustrate that no relevant differences could be detected in the export of R9 and r9 after 30 min and 1 hr, both in MC57 and in HeLa cells. This result indicates that a differential export is also not a likely reason for the observed differences.

Difference in Uptake of Other Cationic L- and D-CPPs in HeLa and MC57 Cells

To investigate whether the differences in uptake were restricted to the polyarginines R9 and its all-D counterpart or were also valid for other types of cell-penetrating peptides, we compared the uptake of the L- and D-forms of the CPPs penetratin and hLF, corresponding to amino acids 38–59 of human lactoferrin (Duchardt et al., 2009), in HeLa and MC57 cells (Figures 2A and 2B). For both of these L-peptides and their D-counterparts, the D-peptides

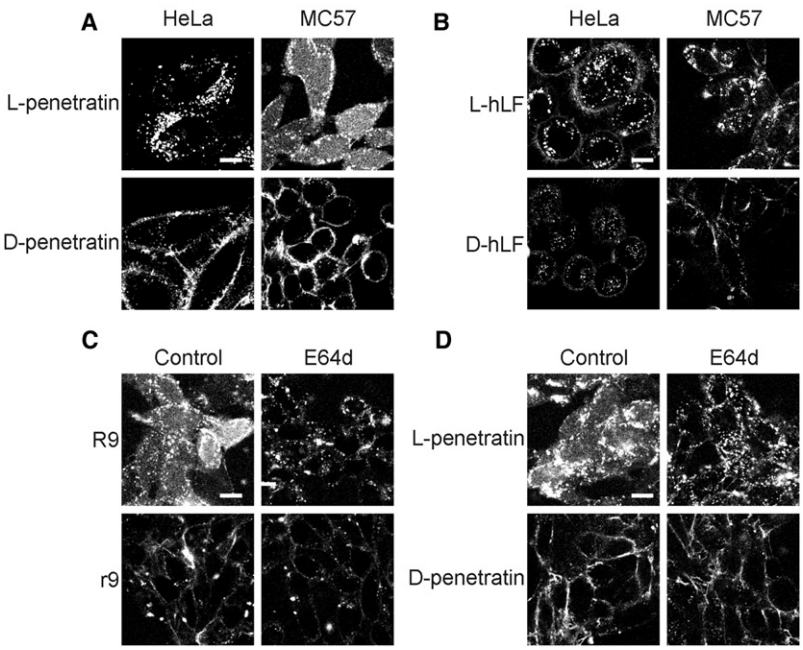

Figure 2. Differences in Uptake Are Observed for Various Different CPPs and Are Not Explained by the Stability of D-Peptides against Cysteine Proteases

(A and B) For all experiments, cells were seeded in eight-well microscopy chambers, grown to 75% confluence, and incubated with 5 μM of each peptide. Cells were washed twice and confocal images were taken immediately. HeLa and MC57 cells were incubated for 45 min with L- or D-penetratin (A) or for 30 min with L- or D-hLF (B). (C and D) MC57 cells were preincubated with 40 μM E-64d before a 45 min CPP incubation in the presence or absence of E-64d with R9 or r9 (C) or with L- or D-penetratin (D).

The scale bars represent 10 μm.

remained much more membrane bound than the L-counterparts in MC57 cells, in agreement with the observations for the nona-arginine peptides. For hLF, membrane-bound fluorescence was observed for both stereoisomers, but endocytosis of D-hLF was clearly reduced, as quantitatively confirmed by measuring the intracellular fluorescence in cell lysates (see below).

Effects of Intracellular Stability on Peptide Localization

Previously, we reported that under conditions where endocytosis was the dominant route of uptake the cytoplasmic fluorescence, but not the vesicular fluorescence, of L-penetratin in MC57 cells was reduced by the broad-range cysteine protease inhibitor E-64d (Fischer et al., 2010). Cysteine proteases of the cathepsin family are a major part of proteolytic activity in the endolysosomal compartment. Therefore, the result indicated that fluorescein-bearing proteolytic fragments escape the endosome more efficiently than intact peptides. We thus reasoned that the differences in distribution of intracellular fluorescence of D- and L-peptides observed by confocal microscopy might be related to the intracellular stability of the peptides. To investigate this possibility, MC57 cells were incubated with E-64d and treated with either R9 or r9. Similar to our previous results, we observed that cytoplasmic fluorescence upon R9 and L-penetratin treatment was completely abolished by E-64d (Figures 2C and 2D). However, vesicular fluorescence was unaffected. Moreover, no effect on the distribution of either D-CPP was apparent. These results indicate that the cytoplasmic fluorescence but not the differences in vesicular fluorescence are related to intracellular CPP stability.

Stimulation of Uptake of Fluorescein-Labeled r9 by Unlabeled R9/r9

We and others had demonstrated that CPPs can actively induce endocytosis (Fotin-Mleczek et al., 2005; Kaplan et al., 2005). We therefore tested whether endocytosis of r9 could be increased by coincubation with unlabeled R9. However, no increased internalization of r9 could be observed (Figure S5A).

Role of HS Chains in Membrane Binding and Cellular Uptake of L- versus D-CPPs

Heparan sulfate chains have been shown to interact with arginine-rich cell-penetrating peptides (Gonçalves et al., 2005; Ziegler and Seelig, 2004) and to play a role in the uptake of CPPs (Nakase et al., 2004; Richard et al., 2005). We therefore hypothesized that binding of peptides to HS chains might contribute to the different uptake of L- and D-peptides. If this was the case, one consequence would be that Jurkat cells, for which no differences in uptake were observed, should expose fewer HS chains on their surface than MC57 and HeLa cells. Furthermore, removal of HS chains by heparinase should reduce the absolute difference in peptide uptake.

In order to test these predictions, first, the presence of HS chains on three cell types was investigated by immunofluorescence. Immunofluorescence staining of all three cell lines was conducted both separately (Figure 3A) and, in order to ensure maximum comparability of signal intensities, also in one sample (Figure 3B). In accordance with our prediction, there was a clear correlation between the presence of HS and the preference for internalization of R9 over r9. HS chains were present on MC57 cells and on HeLa cells, but were undetectable on Jurkat cells.

To further investigate whether the membrane staining of the D-CPPs observed for MC57 and HeLa cells represented peptides binding to HS, MC57 cells were treated with heparinases to remove HS chains from the cell surface (Figure 3C). For r9, heparinase pretreatment of cells abolished membrane-bound fluorescence. Only little punctate fluorescence inside the cells was still observed. For R9, heparinase treatment had very little effect on the distribution of fluorescence. Instead, there was a reduction in the intensity of the cytoplasmic fluorescence, demonstrating a reduction of uptake. In order to quantitatively investigate these differences, cellular peptide uptake in all three cell lines was quantitated by fluorimetry after removal of membrane-bound peptides (Figures 3D–3F). Consistent with the microscopy data, after heparinase treatment a clear trend was visible showing a greater absolute decrease of R9 than r9 in HS-rich MC57 and HeLa cells, and for L-hLF compared to

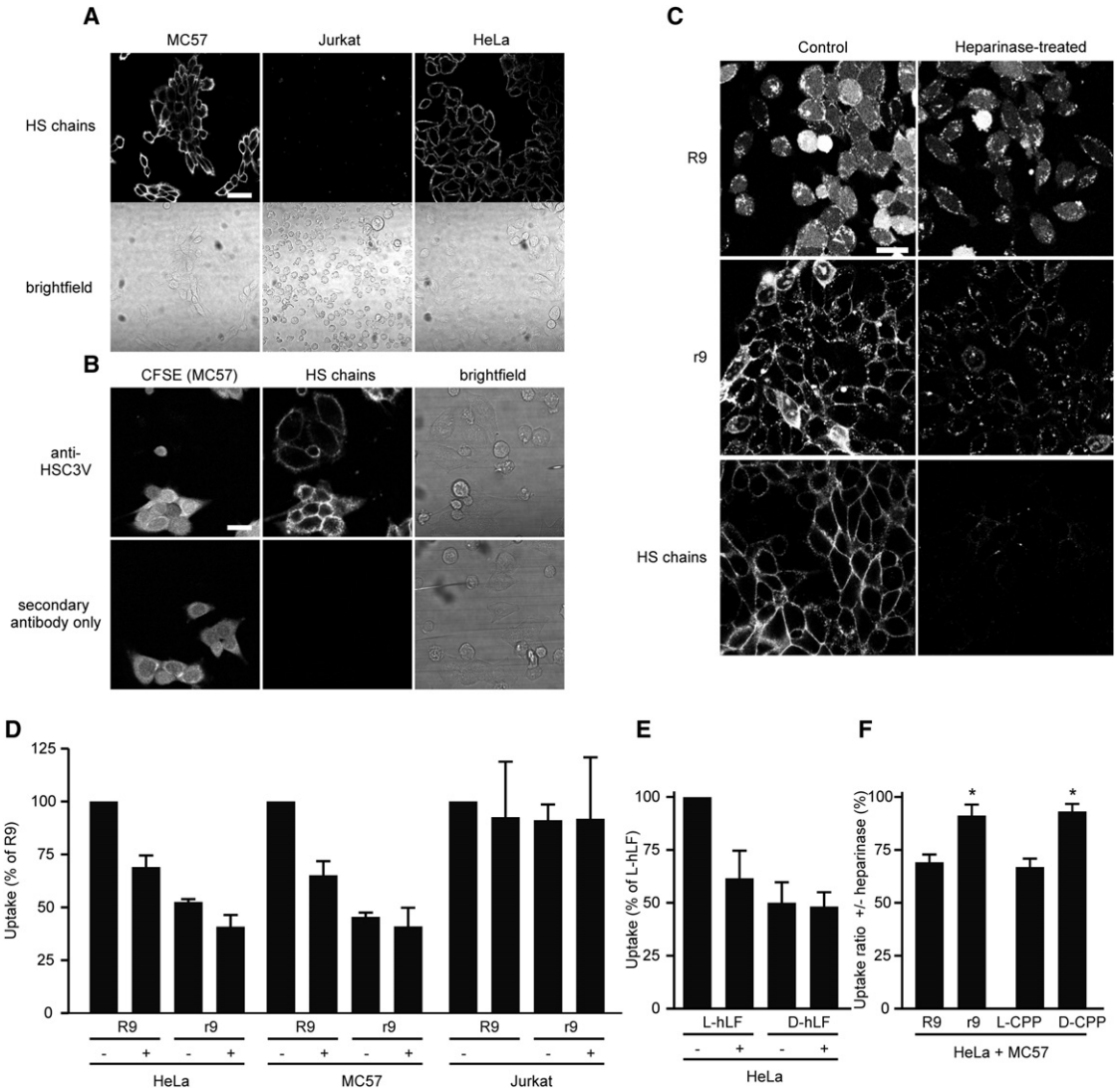

Figure 3. Role of HS Chains in CPP Binding and Uptake

(A) Detection of HS on HeLa, MC57, and Jurkat cells. MC57 cells and HeLa cells were seeded in eight-well microscopy chambers, and Jurkat cells were obtained from a culture flask at the start of the experiment. All three cell lines were probed for HS chains by indirect immunofluorescence of living cells. The scale bar represents 40 μm.

(B) Parallel detection of HS on HeLa, MC57, and Jurkat cells. MC57 cells were distinguished by CFSE labeling and seeded together with HeLa cells in an eight-well microscopy chamber. Jurkat cells were stained according to the same procedure in parallel and seeded in the wells after the final washing steps. Jurkat cells could be detected based on their size and morphology. In the control, only the secondary antibody was applied. The scale bar represents 10 μm.

(C) Effect of HS chain removal on the uptake and distribution of R9 and r9 in MC57 cells. MC57 cells were pretreated with heparinases for 1 hr or left untreated. Cells were washed and incubated with 5 μM indicated peptide for 45 min. HS chains were labeled by indirect immunofluorescence of living cells. The scale bar represents 20 μm.

(D–F) Quantification of the impact of HS chain removal on peptide uptake. HeLa, MC57, and Jurkat cells were pretreated with heparinases (+) for 1 hr to remove HS chains or left untreated (−), washed, and incubated for 45 min with 5 μM of the indicated peptide. Subsequently, cells were washed with heparin to remove membrane-bound peptides, lysed, and centrifuged. Fluorescence in the supernatant was measured using a microplate reader. The fluorescence of R9 (D) and L-hLF (E) in untreated cells was set at 100% to aid comparison with the treated peptides or analogs. In (F), the effect of a heparinase treatment on uptake of R9 and r9 (left bars), and other L-CPPs and D-CPPs (right bars) (analysis includes L/D-penetratin and L/D-hLF), is depicted as the ratio of uptake before and after a heparinase treatment in cells expressing heparan sulfates. Error bars indicate the mean ± SEM. *$p < 0.05$. See also Figure S2.

D-hLF in HeLa cells. A combined statistical analysis of the HS-rich HeLa and MC57 cells demonstrated that the absolute decrease of R9 after heparinase treatment was greater than for r9 ($p < 0.01$). When data for L- and D-hLF were also included in this analysis, the different effects of heparinase treatment on the uptake of L- and D-peptides were even more significant ($p < 0.001$), arguing that the absolute decrease of uptake of L-CPPs was significantly more affected by a heparinase treatment in HS-rich cells. In line with these findings, the effect of HS chain removal on r9 internalization was nonsignificant.

Heparan Sulfate Binding

Having shown that heparan sulfates contribute to the effectiveness of peptide entry, especially of L-peptides, it was still unclear at this point whether heparan sulfates serve as mere attachment factors or as true receptors with an active role in the induction of internalization. The major reason for the inability to directly distinguish between these roles is that both mechanisms would contribute to the effectiveness of peptide entry. Similar practical problems are encountered when trying to distinguish between attachment factors and receptors in elucidating the entry mechanisms of viruses (Mercer et al., 2010).

To probe for differences in the interaction between heparan sulfates and L- and D-CPPs, we first conducted SPR spectroscopy with immobilized heparan sulfate. With SPR, a slightly higher affinity of r9 for HS chains was observed compared to R9, whereas affinities for L- and D-penetratin were very similar (Figures 4A–4D and Table 1). With ITC, too, similar K_D values were obtained for both peptide pairs, although these values differed somewhat from those obtained with SPR (Figures 4E–4H and Table 1). Notably, the stoichiometry, enthalpy (ΔH), and entropy (ΔS), but not the K_D, were changed slightly for r9 compared to R9, indicative of a somewhat different mode of binding. In contrast, for L- and D-penetratin, the contributions of enthalpy and entropy, as well as the stoichiometry and binding affinity, were all very similar. Therefore, it is very unlikely that the slight differences in HS binding observed for R9 and r9 underlie the pronounced differences in behavior of these peptides at the plasma membrane in HeLa and MC57 cells.

Nitric Oxide and Uptake

As a further potential molecular mechanism to explain the differences in the uptake of arginine-containing L- and D-peptides, we examined the involvement of nitric oxide formation. L-arginine released from L-peptides through proteolysis may serve as a substrate for nitric oxide generation by nitric oxide synthase. Nitric oxide is a free radical that can lead to cellular stress and the activation of stress-induced P38, which could in turn stimulate endocytosis (Sorkin and von Zastrow, 2009). Cells were incubated with the nitric oxide synthase inhibitor N(G)-nitro-L-arginine methyl ester (L-NAME). The differences in uptake efficiency that were observed for R9 and r9 were very minor (Figure S5B), indicating the absence of a pivotal role for nitric oxide generation in the differences in uptake of R9 and r9.

Uptake of L/D-Chimeras of Nona-Arginine in MC57 Cells

Having strong indications that L- and D-CPPs differ with respect to triggering their uptake, we were interested to learn more about the structure-activity relationship of this trigger. Therefore, internalization of L/D-chimeras of nona-arginine was assessed in MC57 cells (Figure 5). When only the C- and N-terminal L-amino acids were exchanged for D-amino acids, endocytic internalization still occurred, but cytoplasmic fluorescence was abolished. In contrast, when multiple L-amino acids were mutated to D-amino acids, a persistent membrane binding was observed, resembling the phenotype of r9. These data suggest that a consecutive stretch of L-amino acids is required to trigger efficient endocytic uptake.

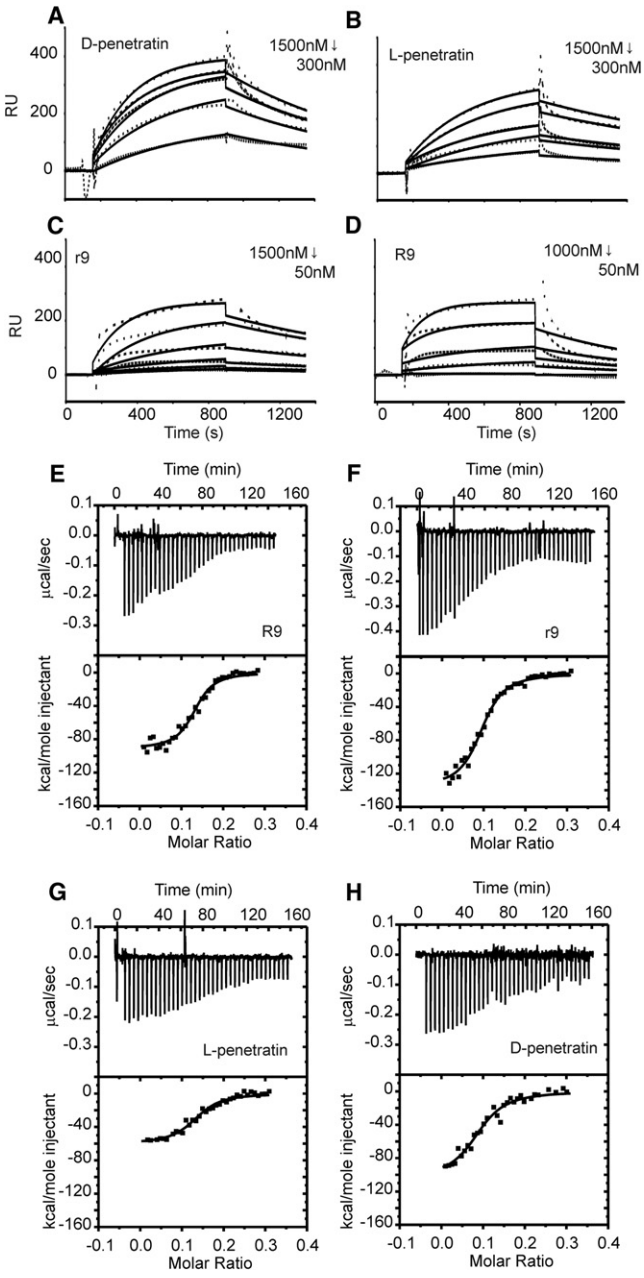

Figure 4. Interaction between HS and L- and D-CPPs as Determined by SPR and ITC

(A–D) SPR diagrams of D- and L-peptide binding to immobilized HS. Peptides and concentration ranges are indicated.

(E–H) ITC of the interaction between HS and L- and D-CPPs. The raw ITC graphs show the reference power as a function of time over the course of a single representative experiment, where 1 µl injections of 30 µM HS were added to 200 µl of 20 µM R9 or r9 in the sample cell. The ITC graphs in the lower panels show the integrated heats per HS injection, expressed as heat per injected mole of HS, as a function of the molar ratio of HS and peptide in the cell.

DISCUSSION

According to the paradigm, chirality does not play a role in the uptake of CPPs. However, here we demonstrate a clear chirality

Table 1. Results of SPR and ITC Binding Studies between HS and L- and D-CPPs

SPR		ITC			
Peptide	K_D (μM)	K_D (μM)	Stoichiometry	ΔH (kcal mol^{-1})	ΔS (kcal mol^{-1} K^{-1})
R9	0.30 ± 0.13	0.14 ± 0.04	8 ± 1	−99 ± 4	−0.32 ± 0.01
r9	0.19 ± 0.06	0.16 ± 0.01	11 ± 1	−129 ± 7	−0.43 ± 0.03
L-penetratin	0.53 ± 0.15	0.15 ± 0.02	10 ± 3	−78 ± 11	−0.25 ± 0.05
D-penetratin	0.48 ± 0.02	0.16 ± 0.03	10 ± 3	−89 ± 9	−0.29 ± 0.03

dependence in the uptake of the arginine-containing CPPs nona-arginine, hLF, and penetratin. Differences in internalization were observed in MC57 and HeLa cells in a concentration range for which endocytosis dominates the uptake of arginine-containing CPPs (Duchardt et al., 2007). No differences were observed in Jurkat cells, in agreement with previous observations (Wender et al., 2000).

The preference for L-peptides was only observed in cells containing significant amounts of heparan sulfates on the plasma membrane. On these cells, D-CPPs of nona-arginine, penetratin, and hLF remained strongly membrane associated, whereas no such prominent association was observed in HeLa cells for the corresponding L-CPPs, except for L-hLF. Also, only in these HS-positive cell types was the internalization of L-CPPs higher compared to D-CPPs. The importance of the chirality of the amino acids was further underscored by the use of two nona-arginine chimeras composed of D- and L-amino acids that showed different phenotypes of internalization, depending on the position and number of D-amino acids. For nona-arginine, HS was identified as an important interaction partner in MC57 cells, as its removal reduced the membrane binding of r9. Additionally, HS chain removal had a greater absolute effect on the internalization of all-L CPPs in comparison to all-D CPPs in MC57 and HeLa cells.

Heparan sulfates have recently been proposed as receptors for arginine-rich peptides (Nakase et al., 2004; Richard et al., 2005). This view is based on the observation that arginine-rich CPPs, upon their interaction with HS proteoglycans, induce actin rearrangements typical for macropinocytosis (Nakase et al., 2004). In our study, SPR and ITC binding assays indicated marginal differences in the binding of the various arginine-containing L- and D-CPPs to HS, supporting the notion that HS serve primarily as attachment factors instead of true receptors in MC57 and HeLa cells. As a consequence, the recognition event at the plasma membrane, which is responsible for the more efficient internalization of L-CPPs versus D-CPPs, remains unknown at present. Because the internalization of L- and D-CPPs was much more similar after removal of HS chains, it is reasonable to speculate that the presence of HS chains strongly facilitates this unknown interaction. One prominent possibility is the presence of a protein receptor that carries HS chains, such as the recently proposed syndecan-4 (Letoha et al., 2010). An involvement of a protein factor associated with internalization of CPPs is supported by studies in CHO cells, in which the selective removal of glycosaminoglycans only partially reduced internalization, whereas trypsin treatment almost completely abolished internalization via endocytosis (Gump et al., 2010). A distinction between binding and internalization has also recently been observed for HS chain-directed single-chain variable-domain antibody fragments (scFv). Only one scFv of several tested was efficiently internalized, whereas others remained membrane bound (Wittrup et al., 2009). Remarkably, we were not able to stimulate uptake of labeled r9 by the addition of unlabeled R9, even though it had been previously shown that CPPs can actively induce endocytosis (Fotin-Mleczek et al., 2005; Kaplan et al., 2005). These data indicate that both isomers behave as distinct molecular entities at the plasma membrane. Interestingly, similar results were reported for the induction of nucleation zone-dependent uptake (Tünnemann et al., 2008).

Intracellular degradation (Fischer et al., 2004, 2010; Hällbrink et al., 2004) and reexport (Oehlke et al., 1998) have been shown to affect the cellular distribution and intracellular retention time of CPPs. Moreover, the sensitivity of the fluorescence of the fluorescein moiety to the chemical environment, for example pH or hydrophobicity, and to collision quenching with neighboring groups is well known. In addition, careful preparation of lysates is an important factor when comparing numbers of fluorophores from intact D- and (partially) degraded L-peptides. In our experiments, we could exclude all of these factors as a source of the observed differences. However, the cytoplasmic fluorescence observed after treatment of cells with L-peptides under conditions where endocytosis is the dominant route of uptake very likely relates to their proteolytic sensitivity, as R9- or L-penetratin-incubated cells were devoid of cytoplasmic fluorescence after pretreatment with the endolysosomal protease inhibitor E-64d (Figure 2). We had previously reported the same observation for L-penetratin (Fischer et al., 2010). Quite remarkably, the internalization pattern of an R9 analog with terminal D-amino acids reflected the same pattern observed with R9 after pretreatment with E-64d. We thus conclude that the terminal D-amino acids were sufficient to inhibit proteolysis in endocytic vesicles, whereas the central stretch of seven consecutive L-amino acids was sufficient to induce endocytosis effectively.

Extracellular peptide degradation is also a very unlikely cause of differences in the internalization, as shorter oligo-arginine fragments (<R9) are taken up with a considerably lower efficiency (Wender et al., 2000). Regarding the heparin treatment we used, it may not have removed membrane-bound peptides completely, but this would only have led to an overestimation of the internalization of D-peptides.

The reason for the higher proportion of HeLa cells showing internalization of r9 via direct translocation is not necessarily a consequence of a greater stability toward proteolytic activity. Instead, the reduction of internalization via endocytosis might accelerate accumulation of peptide at the plasma membrane, which might trigger direct translocation more rapidly. Consistent with this hypothesis, the concentration threshold at which the

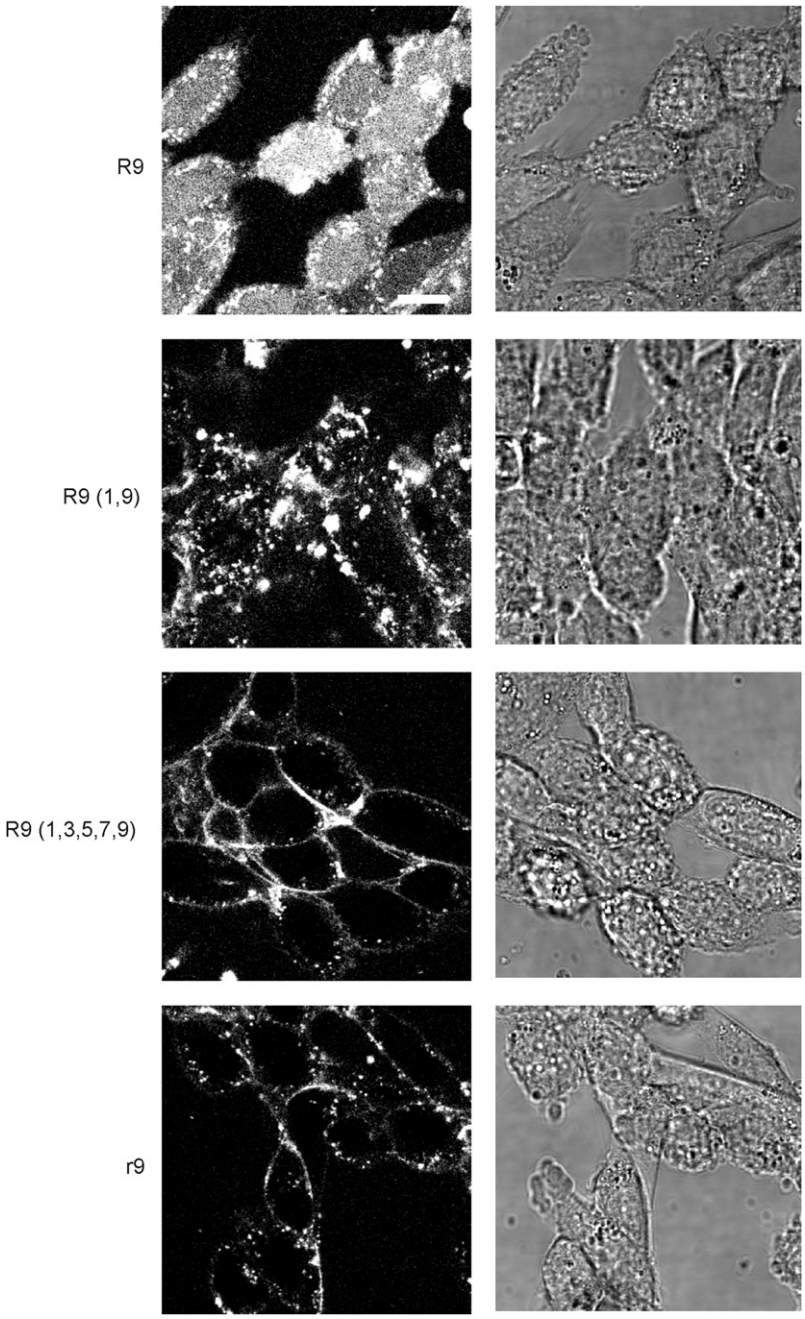

Figure 5. Uptake of R9, r9, and Nona-Arginine Chimeras Composed of L- and D-Amino Acids in MC57 Cells

Cells were seeded in eight-well microscopy chambers, grown to 75% confluence, and incubated with 5 μM of the indicated peptides for 45 min. Cells were washed twice and confocal images were taken immediately. The scale bar represents 10 μm. See also Figure S5.

direct translocation occurs could be lowered by incubation of cells with endocytosis inhibitors (Duchardt et al., 2007).

Even though our results clearly refute the earlier paradigm of a chirality-independent uptake of CPPs, our results do not contradict earlier findings. Instead, prior experiments had been designed in such a way that they missed these differences. In accordance with previous findings, we did not detect a difference in the uptake of R9 and r9 in Jurkat cells (Wender et al., 2000). When Tünnemann et al. compared the uptake of R9 and r9, they only focused on the number of cells that showed rapid translocation across the membrane (Tünnemann et al., 2008).

It should also be pointed out that differences were previously reported for molecular complexes containing L- and D-CPPs. Mason et al. found a reduced transfection efficiency for DNA complexes containing the amphipathic peptide D-LAH4 compared to L-LAH3 (Mason et al., 2007), and Abes et al. found a reduced biological activity of morpholino-oligomer-peptide complexes with partial D-amino acid substitutions (Abes et al., 2008). Remarkably, retro-inverso CPPs were much more toxic to cells, demonstrating that despite very similar side-chain orientations, these peptides also induced very different biological responses (Holm et al., 2011). Although these studies indicate a different behavior for peptides containing D-amino acids, none of these studies had explicitly addressed the impact of chirality on internalization efficiency.

Taken together, our findings indicate that cell-surface binding and the induction of internalization are distinct mechanisms with individual structure-activity relationships. For the CPPs nona-arginine, penetratin, and the hLF peptide, our data indicate that binding to heparan sulfates is chirality independent, whereas the efficiency of internalization is related to chirality. We envision that these findings will have important consequences for the use of L- and D-amino acids in drug delivery strategies in general.

The cell line dependence of our results also suggests a potential to employ the HS-dependent discrimination of CPPs for tissue-selective targeting. The preferential uptake of arginine-containing L-CPPs by cells expressing HS may be exploited for a preferential targeting of these cells. Conversely, targeting to cells not expressing HS can be more easily accomplished with CPPs synthesized with D-amino acids.

SIGNIFICANCE

Cell-penetrating peptides (CPPs) represent a class of short, usually cationic peptides that efficiently induce cellular uptake of large membrane-impermeable macromolecules. However, an important factor limiting the pharmacological potential of CPPs is their proteolytic instability, which can be overcome through incorporation of D-amino acids.

Contrary to the current paradigm, our results show clear differences in the uptake efficiency of the L- and D-form of three arginine-containing CPPs. These differences can be understood in terms of a two-step internalization process of CPPs at low concentrations: first, binding to heparan sulfates (HS) on the plasma membrane; second, internalization by endocytosis. Our data indicate that in the presence of HS chains only the second step occurs less efficiently for D-CPPs and can therefore be considered chirality dependent. Data supporting this hypothesis include (1) the correlation of a more efficient internalization of L-CPPs with the expression of HS, and (2) the pronounced membrane fluorescence of D-CPPs, but not L-CPPs, in HS-expressing cells, which can be eliminated by a heparinase treatment. Moreover, HS removal affects mainly the internalization of L-CPPs in cell lines with high levels of HS. We could exclude alternative interpretations of the observed differences through a comprehensive set of control experiments. Even though our results disagree with the current paradigm of an equal efficiency of L- and D-CPPs, our results do not contradict any published findings, as these previous results addressed differences for only a limited set of conditions. For in vivo applications, the balance of in vivo proteolytic stability, cellular internalization efficiency, and intracellular trafficking may ultimately be decisive. Results obtained for chimeric L/D-peptides revealed an interesting structure-activity relationship. It will be interesting to explore to what degree such peptides containing only a few D-amino acids may combine the high stability of all-D CPPs with the higher uptake of arginine-containing all-L CPPs.

EXPERIMENTAL PROCEDURES

Materials

All-L and all-D peptides were purchased from EMC Microcollections. Chimeric peptides (R9 [1,9] and R9 [1,3,5,7,9]) were synthesized using standard Fmoc/OtBu solid-phase peptide synthesis protocols on a rink amide resin. Each amino acid was coupled using HOBt/HBTU in the presence of *N*,*N*′-diisopropylethylamine (DIPEA) as a base. Peptides were cleaved from the resin using TFA:triisopropylsilane:H_2O (92.5:5:2.5, v:v:v) and the crude peptides were purified on C18 reverse-phase HPLC columns using water/acetonitrile gradients. N-terminal fluorophore labeling was performed using 5(6)-carboxyfluorescein as previously described (Fischer et al., 2003). Peptides were synthesized C-terminally amidated and N-terminally fluorescein labeled, unless stated otherwise. Purity was evaluated by analytical HPLC and identity was confirmed by mass spectrometry. hLF peptides were oxidized by purging oxygen through the peptide solution for 5 min, followed by a 2 hr incubation at 37°C. Oxidation leads to cyclization by disulfide-bridge formation.

The Zenon mouse IgG1 labeling kit was from Invitrogen; BSA, octyl-β-D-glucopyranoside, heparin, and glucose were from Sigma-Aldrich. Heparan sulfate (average MW 15 kDa) was from Celsus. Heparinases I–III were purchased from IBEX. The anti-HS VSV-tagged single-chain Fv fragment HS4C3V was described previously (van Kuppevelt et al., 1998), and the mouse anti-VSV (clone P5D4) antibody was from Boehringer Mannheim. E-64d was from Bachem. Standard chemicals were from Sigma-Aldrich and Merck.

Cell Culture

All cell lines were maintained in RPMI 1640 (PAN Biotech) supplemented with 10% heat-inactivated fetal calf serum (PAN Biotech) and passaged every 2–3 days. Cells were incubated at 37°C in a 5% CO_2, humidified incubator.

Confocal Laser-Scanning Microscopy and Fluorescence-Correlation Spectroscopy

Confocal laser-scanning microscopy and FCS were performed on a TCS SP5 confocal microscope (Leica Microsystems) equipped with an HCX PL APO 63× NA 1.2 water immersion lens and a dual-channel FCS unit. Fluorescein fluorescence was excited with the 488 nm line of an argon ion laser. Detection took place with a 500–550 nm filter block for FCS measurements and with a 500–550 nm detection range for confocal microscopy. Cells were maintained at 37°C on a temperature-controlled microscope stage.

Peptide Uptake

MC57 and HeLa cells were seeded in eight-well microscopy chambers (Nunc) and grown to 75% confluence. Jurkat cells were transferred from the tissue culture flask immediately before the experiment. Cells were incubated at 37°C with 5 μM peptides in RPMI 1640 supplemented with 10% fetal calf serum. The duration of incubations is indicated for each experiment separately. Cells were washed twice with medium after the incubation with peptides, and living cells were analyzed immediately or after settling for about 15 min in the microscopy chambers (Jurkat cells) by confocal microscopy. Removal of HS chains from the cell surface was accomplished by a 1 hr incubation at 37°C with RPMI 1640 supplemented with 1% fetal calf serum, 33 mIU/ml of heparinase I, 8 mIU/ml of heparinase II, and 5 mIU/ml of heparinase III.

Quantification of Cellular Uptake

After incubation with the peptides, cells were washed with prewarmed HEPES-buffered saline (HBS)/BSA/glucose (10 mM HEPES, 135 mM NaCl, 5 mM KCl, 1 mM $MgCl_2$, 1.8 mM $CaCl_2$ [pH 7.4], containing 0.1% [w/v] BSA and 5 mM glucose), treated twice for 5 min at 37°C with 100 μg/ml heparin in HBS/BSA/glucose, and washed again with HBS/BSA/glucose. Cells were then lysed in 150 μl lysis buffer (10 mM bis-Tris propane, 50 mM octyl-β-D-glucopyranoside, 1 mM EDTA, and 150 mM NaCl [pH 7.2]) for 15 min on ice; the lysate was centrifuged for 10 min at 18,000 × *g* and the fluorescence in 120 μl of the supernatant was measured using a Synergy 2 microplate reader (Biotek) by excitation at 488 ± 10 nm and detection at 528 ± 10 nm in a flat-bottom 96-well plate (Nunc). Values were corrected for total protein content on the basis of results from the Bio-Rad protein assay in microtiter plates with the dye reagent from Bio-Rad. For quantification by FCS, 150 μl of lysate was treated with 2 μl of benzonuclease (2U; Novagen, Merck) for 30 min at 37°C, followed by a 3 hr incubation with 3.3 mg/ml proteinase K (diluted from a 20 mg/ml stock; Roche) at 37°C. For a detailed description of the FCS analysis, please refer to Supplemental Experimental Procedures.

Immunofluorescence

Cells were washed with ice-cold HBS/BSA/glucose and incubated with 125 μl of a periplasmic fraction containing the anti-HS single-chain Fv fragment HS4C3V for 1 hr on ice in eight-well microscopy chambers (MC57 and HeLa cells) or in the same volume in Eppendorf tubes (800,000 Jurkat cells). After incubation, cells were washed again with ice-cold HBS/BSA/glucose and incubated for 1 hr with an anti-VSV antibody (P5D4)/Zenon IgG1-Alexa Fluor 647 conjugate on ice. The antibody staining was analyzed by confocal microscopy. When coseeding MC57, HeLa, and Jurkat cells, MC57 cells were distinguished from HeLa cells using the Celltrace carboxyfluorescein diacetate succinimidylester (CFSE) proliferation kit (Molecular Probes, Invitrogen) according to the manufacturer's instructions.

Pulse-Chase Experiment

MC57 and HeLa cells were detached by trypsinization for 5 min and incubated with prewarmed RPMI 1640 supplemented with 10% fetal calf serum. One million cells were mixed with 5 μM indicated peptide and immediately electroporated using the Amaxa nucleofector kit R (Lonza), according to the manufacturer's instructions. After electroporation, cells were washed twice with medium and 125,000 cells per well were seeded in eight-well microscopy chambers. Confocal images were taken 30 min and 1 hr after electroporation. Mean intracellular fluorescence was quantitated using the ImageJ software package (http://rsb.info.nih.gov/ij).

Flow Cytometry

HeLa cells were seeded in 24-well plates (Sarstedt) at a density of 40,000 cells/well 2 days prior to the experiment. For experiments probing for an involvement of NO synthase in uptake differences, cells were incubated for 30 min with or without 200 μM L-NAME in RPMI 1640 without serum followed by a 30 min incubation with 5 or 10 μM R9 in the presence or absence of 200 μM L-NAME in serum-containing RPMI. Subsequently, cells were washed, detached by trypsinization for 5 min, spun down, and resuspended in 200 μl HBS, and cellular fluorescence was measured using a BD FACScan flow cytometer equipped with a 488 nm laser (BD Biosciences). The analysis was performed using Summit software (Dako). Results were based on 10,000 gated cells.

Surface Plasmon Resonance and Isothermal Titration Calorimetry

SPR and ITC were performed on a Biacore 2000 (GE Healthcare) and an ITC_{200} system (MicroCal), respectively. For detailed protocols regarding these techniques, see Supplemental Experimental Procedures.

SUPPLEMENTAL INFORMATION

Supplemental Information includes five figures, one table, and Supplemental Experimental Procedures and can be found with this article online at doi:10.1016/j.chembiol.2011.06.006.

ACKNOWLEDGMENTS

We thank I.R. Ruttekolk for support with FCS measurements. The authors acknowledge financial support from the Volkswagen Foundation (Nachwuchsgruppen an Universitäten, I/77 472) and from the Radboud University Nijmegen Medical Centre. The funders had no role in study design, data collection and analysis, decision to publish, or preparation of the manuscript. The authors declare no competing financial interests.

Received: December 22, 2009
Revised: June 3, 2011
Accepted: June 10, 2011
Published: August 25, 2011

REFERENCES

Abes, R., Moulton, H.M., Clair, P., Yang, S.T., Abes, S., Melikov, K., Prevot, P., Youngblood, D.S., Iversen, P.L., Chernomordik, L.V., and Lebleu, B. (2008). Delivery of steric block morpholino oligomers by (R-X-R)4 peptides: structure-activity studies. Nucleic Acids Res. *36*, 6343–6354.

Al-Taei, S., Penning, N.A., Simpson, J.C., Futaki, S., Takeuchi, T., Nakase, I., and Jones, A.T. (2006). Intracellular traffic and fate of protein transduction domains HIV-1 TAT peptide and octaarginine. Implications for their utilization as drug delivery vectors. Bioconjug. Chem. *17*, 90–100.

Brugidou, J., Legrand, C., Méry, J., and Rabié, A. (1995). The retro-inverso form of a homeobox-derived short peptide is rapidly internalised by cultured neurones: a new basis for an efficient intracellular delivery system. Biochem. Biophys. Res. Commun. *214*, 685–693.

Burlina, F., Sagan, S., Bolbach, G., and Chassaing, G. (2005). Quantification of the cellular uptake of cell-penetrating peptides by MALDI-TOF mass spectrometry. Angew. Chem. Int. Ed. Engl. *44*, 4244–4247.

Derossi, D., Calvet, S., Trembleau, A., Brunissen, A., Chassaing, G., and Prochiantz, A. (1996). Cell internalization of the third helix of the Antennapedia homeodomain is receptor-independent. J. Biol. Chem. *271*, 18188–18193.

Duchardt, F., Fotin-Mleczek, M., Schwarz, H., Fischer, R., and Brock, R. (2007). A comprehensive model for the cellular uptake of cationic cell-penetrating peptides. Traffic *8*, 848–866.

Duchardt, F., Ruttekolk, I.R., Verdurmen, W.P., Lortat-Jacob, H., Bürck, J., Hufnagel, H., Fischer, R., van den Heuvel, M., Löwik, D.W., Vuister, G.W., et al. (2009). A cell-penetrating peptide derived from human lactoferrin with conformation-dependent uptake efficiency. J. Biol. Chem. *284*, 36099–36108.

Elmquist, A., and Langel, U. (2003). In vitro uptake and stability study of pVEC and its all-D analog. Biol. Chem. *384*, 387–393.

Fischer, R., Mader, O., Jung, G., and Brock, R. (2003). Extending the applicability of carboxyfluorescein in solid-phase synthesis. Bioconjug. Chem. *14*, 653–660.

Fischer, R., Köhler, K., Fotin-Mleczek, M., and Brock, R. (2004). A stepwise dissection of the intracellular fate of cationic cell-penetrating peptides. J. Biol. Chem. *279*, 12625–12635.

Fischer, R., Hufnagel, H., and Brock, R. (2010). A doubly labeled penetratin analogue as a ratiometric sensor for intracellular proteolytic stability. Bioconjug. Chem. *21*, 64–73.

Fotin-Mleczek, M., Welte, S., Mader, O., Duchardt, F., Fischer, R., Hufnagel, H., Scheurich, P., and Brock, R. (2005). Cationic cell-penetrating peptides interfere with TNF signalling by induction of TNF receptor internalization. J. Cell Sci. *118*, 3339–3351.

Fretz, M.M., Penning, N.A., Al-Taei, S., Futaki, S., Takeuchi, T., Nakase, I., Storm, G., and Jones, A.T. (2007). Temperature-, concentration- and cholesterol-dependent translocation of L- and D-octa-arginine across the plasma and nuclear membrane of $CD34^+$ leukaemia cells. Biochem. J. *403*, 335–342.

Gonçalves, E., Kitas, E., and Seelig, J. (2005). Binding of oligoarginine to membrane lipids and heparan sulfate: structural and thermodynamic characterization of a cell-penetrating peptide. Biochemistry *44*, 2692–2702.

Gump, J.M., June, R.K., and Dowdy, S.F. (2010). Revised role of glycosaminoglycans in TAT protein transduction domain-mediated cellular transduction. J. Biol. Chem. *285*, 1500–1507.

Hällbrink, M., Oehlke, J., Papsdorf, G., and Bienert, M. (2004). Uptake of cell-penetrating peptides is dependent on peptide-to-cell ratio rather than on peptide concentration. Biochim. Biophys. Acta *1667*, 222–228.

Holm, T., Räägel, H., Andaloussi, S.E., Hein, M., Mäe, M., Pooga, M., and Langel, U. (2011). Retro-inversion of certain cell-penetrating peptides causes severe cellular toxicity. Biochim. Biophys. Acta *1808*, 1544–1551.

Hosaka, Y., Yasuda, Y., Seriburi, O., Moran, M.G., and Fukai, K. (1986). In vitro secondary generation of cytotoxic T lymphocytes in mice with mumps virus and their mumps-specific cytotoxicity among paramyxoviruses. J. Virol. *57*, 1113–1118.

Järver, P., Mäger, I., and Langel, U. (2010). In vivo biodistribution and efficacy of peptide mediated delivery. Trends Pharmacol. Sci. *31*, 528–535.

Kaplan, I.M., Wadia, J.S., and Dowdy, S.F. (2005). Cationic TAT peptide transduction domain enters cells by macropinocytosis. J. Control. Release *102*, 247–253.

Kosuge, M., Takeuchi, T., Nakase, I., Jones, A.T., and Futaki, S. (2008). Cellular internalization and distribution of arginine-rich peptides as a function of extracellular peptide concentration, serum, and plasma membrane associated proteoglycans. Bioconjug. Chem. *19*, 656–664.

Letoha, T., Keller-Pintér, A., Kusz, E., Kolozsi, C., Bozsó, Z., Tóth, G., Vizler, C., Oláh, Z., and Szilák, L. (2010). Cell-penetrating peptide exploited syndecans. Biochim. Biophys. Acta *1798*, 2258–2265.

Lindgren, M.E., Hällbrink, M.M., Elmquist, A.M., and Langel, U. (2004). Passage of cell-penetrating peptides across a human epithelial cell layer in vitro. Biochem. J. *377*, 69–76.

Mason, A.J., Leborgne, C., Moulay, G., Martinez, A., Danos, O., Bechinger, B., and Kichler, A. (2007). Optimising histidine rich peptides for efficient DNA delivery in the presence of serum. J. Control. Release *118*, 95–104.

Mercer, J., Schelhaas, M., and Helenius, A. (2010). Virus entry by endocytosis. Annu. Rev. Biochem. *79*, 803–833.

Mitchell, D.J., Kim, D.T., Steinman, L., Fathman, C.G., and Rothbard, J.B. (2000). Polyarginine enters cells more efficiently than other polycationic homopolymers. J. Pept. Res. *56*, 318–325.

Mueller, J., Kretzschmar, I., Volkmer, R., and Boisguerin, P. (2008). Comparison of cellular uptake using 22 CPPs in 4 different cell lines. Bioconjug. Chem. *19*, 2363–2374.

Nakase, I., Niwa, M., Takeuchi, T., Sonomura, K., Kawabata, N., Koike, Y., Takehashi, M., Tanaka, S., Ueda, K., Simpson, J.C., et al. (2004). Cellular

uptake of arginine-rich peptides: roles for macropinocytosis and actin rearrangement. Mol. Ther. *10*, 1011–1022.

Oehlke, J., Scheller, A., Wiesner, B., Krause, E., Beyermann, M., Klauschenz, E., Melzig, M., and Bienert, M. (1998). Cellular uptake of an α-helical amphipathic model peptide with the potential to deliver polar compounds into the cell interior non-endocytically. Biochim. Biophys. Acta *1414*, 127–139.

Palm, C., Jayamanne, M., Kjellander, M., and Hällbrink, M. (2007). Peptide degradation is a critical determinant for cell-penetrating peptide uptake. Biochim. Biophys. Acta *1768*, 1769–1776.

Patel, L.N., Zaro, J.L., and Shen, W.C. (2007). Cell penetrating peptides: intracellular pathways and pharmaceutical perspectives. Pharm. Res. *24*, 1977–1992.

Pujals, S., Sabidó, E., Tarragó, T., and Giralt, E. (2007). All-D proline-rich cell-penetrating peptides: a preliminary in vivo internalization study. Biochem. Soc. Trans. *35*, 794–796.

Pujals, S., Fernández-Carneado, J., Ludevid, M.D., and Giralt, E. (2008). D-SAP: a new, noncytotoxic, and fully protease resistant cell-penetrating peptide. ChemMedChem *3*, 296–301.

Richard, J.P., Melikov, K., Vives, E., Ramos, C., Verbeure, B., Gait, M.J., Chernomordik, L.V., and Lebleu, B. (2003). Cell-penetrating peptides. A reevaluation of the mechanism of cellular uptake. J. Biol. Chem. *278*, 585–590.

Richard, J.P., Melikov, K., Brooks, H., Prevot, P., Lebleu, B., and Chernomordik, L.V. (2005). Cellular uptake of unconjugated TAT peptide involves clathrin-dependent endocytosis and heparan sulfate receptors. J. Biol. Chem. *280*, 15300–15306.

Ruttekolk, I.R., Verdurmen, W.P., Chung, Y.D., and Brock, R. (2011). Measurements of the intracellular stability of CPPs. Methods Mol. Biol. *683*, 69–80.

Sorkin, A., and von Zastrow, M. (2009). Endocytosis and signalling: intertwining molecular networks. Nat. Rev. Mol. Cell Biol. *10*, 609–622.

Tréhin, R., Nielsen, H.M., Jahnke, H.G., Krauss, U., Beck-Sickinger, A.G., and Merkle, H.P. (2004). Metabolic cleavage of cell-penetrating peptides in contact with epithelial models: human calcitonin (hCT)-derived peptides, Tat(47–57) and penetratin(43–58). Biochem. J. *382*, 945–956.

Tugyi, R., Uray, K., Iván, D., Fellinger, E., Perkins, A., and Hudecz, F. (2005). Partial D-amino acid substitution: improved enzymatic stability and preserved Ab recognition of a MUC2 epitope peptide. Proc. Natl. Acad. Sci. USA *102*, 413–418.

Tünnemann, G., Ter-Avetisyan, G., Martin, R.M., Stöckl, M., Herrmann, A., and Cardoso, M.C. (2008). Live-cell analysis of cell penetration ability and toxicity of oligo-arginines. J. Pept. Sci. *14*, 469–476.

van Kuppevelt, T.H., Dennissen, M.A., van Venrooij, W.J., Hoet, R.M., and Veerkamp, J.H. (1998). Generation and application of type-specific anti-heparan sulfate antibodies using phage display technology. Further evidence for heparan sulfate heterogeneity in the kidney. J. Biol. Chem. *273*, 12960–12966.

Verdurmen, W.P., Thanos, M., Ruttekolk, I.R., Gulbins, E., and Brock, R. (2010). Cationic cell-penetrating peptides induce ceramide formation via acid sphingomyelinase: implications for uptake. J. Control. Release *147*, 171–179.

Wender, P.A., Mitchell, D.J., Pattabiraman, K., Pelkey, E.T., Steinman, L., and Rothbard, J.B. (2000). The design, synthesis, and evaluation of molecules that enable or enhance cellular uptake: peptoid molecular transporters. Proc. Natl. Acad. Sci. USA *97*, 13003–13008.

Wittrup, A., Zhang, S.H., ten Dam, G.B., van Kuppevelt, T.H., Bengtson, P., Johansson, M., Welch, J., Mörgelin, M., and Belting, M. (2009). ScFv antibody-induced translocation of cell-surface heparan sulfate proteoglycan to endocytic vesicles: evidence for heparan sulfate epitope specificity and role of both syndecan and glypican. J. Biol. Chem. *284*, 32959–32967.

Youngblood, D.S., Hatlevig, S.A., Hassinger, J.N., Iversen, P.L., and Moulton, H.M. (2007). Stability of cell-penetrating peptide-morpholino oligomer conjugates in human serum and in cells. Bioconjug. Chem. *18*, 50–60.

Ziegler, A., and Seelig, J. (2004). Interaction of the protein transduction domain of HIV-1 TAT with heparan sulfate: binding mechanism and thermodynamic parameters. Biophys. J. *86*, 254–263.

